International Immunopharmacology 77 (2019) 105944

Contents lists available at ScienceDirect

International Immunopharmacology

journal homepage: www.elsevier.com/locate/intimp

Necroptosis in pulmonary macrophages mediates lipopolysaccharide-induced lung inflammatory injury by activating ZBP-1

Xue-ke Du, Wang-yun Ge, Ren Jing*, Ling-hui Pan*

Department of Anesthesiology, Tumor Hospital of Guangxi Medical University, Nanning, China
Laboratory of Perioperative Medicine Research, Tumor Hospital of Guangxi Medical University, Nanning, Guangxi 530021, China

ARTICLE INFO

Keywords:
ZBP-1
mitochondrial DNA
Necroptosis
Lipopolysaccharide-induced lung injury

ABSTRACT

Z-DNA combined protein-1 (ZBP-1), an important necroptosis regulator, activates necrosis-associated inflammation and immune response. Increased ZBP-1 expression in necroptosis-associated inflammation correlates with activation of receptor interacting protein kinase (RIPK1)/RIPK3 and nuclear factor (NF)-κB. Here we explored the role of ZBP-1-mediated necroptosis in lipopolysaccharide (LPS)-induced lung injury. Bone marrow-derived macrophages (BMDMs) transfected with a small interfering RNA against ZBP-1 or scrambled control RNA were administered to mice that had been depleted of alveolar macrophages (AMs). Then the animals were treated with *E. coli* LPS (2.0 mg/kg) or phosphate-buffered saline by intratracheal instillation for 48 h. LPS-induced lung inflammatory injury was verified, and the mRNA and protein expression of ZBP-1, RIPK1/RIPK3 and NF-κB in AMs were then assessed by Western blot and real time-quantitative polymerase chain reaction. In mechanistic studies *in vitro*, BMDM cultures were treated with different concentrations of LPS for 24 h, and the expression of ZBP-1, RIPK1/RIPK3 and NF-κB were assessed. LPS activated ZBP-1-mediated necroptosis, primarily in AMs. This activation and associated lung inflammatory injury were much weaker after AMs depletion or silencing of ZBP-1 in BMDMs, which correlated with down-regulation of RIPK1/RIPK3. These *in vivo* findings were confirmed in experiments with cultures of BMDMs. In conclusion, LPS induces lung inflammation and injury by activating ZBP-1-mediated necroptosis and release of pro-inflammatory cytokines by macrophages.

1. Introduction

Lipopolysaccharides (LPS) in the outer cell wall of Gram-negative bacteria are highly pro-inflammatory molecules that cause lung injury by inducing inflammation and oxidative stress [4]. In sepsis, for example, endotoxin LPS can cause acute lung injury (ALI) involving hypoxemia, bilateral lung injury, severe diffuse failure of pulmonary ventilation and non-cardiogenic pulmonary edema [3,15]. LPS activate Toll-like receptor 4 signaling and induce the translocation of factor-κB (NF-κB) to the nucleus, where it up-regulates pro-inflammatory cytokines including tumor necrosis factor (TNF)-α, interleukins (IL)-6 and IL-1β [8,12,26]. LPS also trigger the pro-inflammatory cascade response in immune cells such as monocytes, neutrophils and endothelial cells [5].

ALI is driven by various types of cell death: apoptosis, autophagy and necroptosis. Necroptosis is caspase-independent cell death involving necrosis and apoptosis [16]. In contrast to apoptosis and autophagy, necroptosis leads to rupture of the cell membrane and release of cellular contents, which activate inflammation [7,10]. By activating inflammation, necroptosis is associated with heart failure, acute pancreatitis and other inflammatory diseases in animal studies [1,6,17]. The driver of necroptosis is Z-DNA binding protein 1 (ZBP-1), which may play a role in antiviral immunity. ZBP-1 acts an important molecular to activate necroptosis, which would be aborted via the receptor interacting protein kinase 1 (RIPK1) [18,21]. ZBP-1 and RIPK3/mixed lineage kinase domain-like protein (MLKL) activate necroptosis, which can cause epithelial inflammation of lungs [27].

Previous work from our group [9,14] linked mechanical ventilator-induced lung injury with inflammation caused by the release of mitochondrial DNA (mtDNA) during mitophagy. Endogenous mtDNA is recently considered to be a novel intracellular damage-associated molecule pattern [23], Oka T and his colleagues reported that escaped mtDNA during mitophagy can be recognized and combined with Toll-like receptor 9 to cascade inflammation in cardiomyocytes during heart failure [19]. In the present study, we examined whether this mtDNA release might work together with ZBP-1 to trigger necroptosis in LPS-induced lung injury.

* Corresponding authors at: Department of Anesthesiology, Tumor Hospital of Guangxi Medical University, He Di Rd No. 71, Nanning 530021, China.
E-mail addresses: duxueke@gxmu.edu.cn (X.-k. Du), jingren890323@outlook.com (R. Jing), plinghui@hotmail.com (L.-h. Pan).

https://doi.org/10.1016/j.intimp.2019.105944
Received 1 July 2019; Received in revised form 15 September 2019; Accepted 26 September 2019
Available online 23 October 2019

2. Materials and methods

2.1. Animals

Wild type C57BL/6J male mice were purchased from the Animal Center of Guangxi Medical University (Nanning, China) (certificate no. SCXK-Gui-2015-0002), and approved by the Institutional Animal Care and Use Committee of Guangxi Medical University. Mice were housed in squirrel cages under specific pathogen-free conditions, fed with water and autoclaved food, and used in experiments at 8–12 wk of age.

2.2. Depletion of macrophages in mice

Mice were depleted of alveolar macrophages as described [30]. Briefly, clodronate liposomes were prepared by mixing phosphatidylserine, cholesterol and phosphatidylcholine in a molar ratio of 1:4:6 in chloroform. The chloroform was removed by rotary evaporation at 100 rpm at 40 °C, and the liposome solution was passed through 200-nm filters and delivered by nebulization to mice that had been anesthetized by intraperitoneal injection of 90 mg/kg ketamine (Ketalar, Pfizer, Istanbul, Turkey).

2.3. Isolation and culture of bone marrow-derived macrophages (BMDMs) from mice

BMDMs were generated from femurs of C57/BL6J mice as described [30]. Animals were sacrificed by rapid cervical dislocation, and bone marrow was flushed out of the femur using 2–5 ml of phosphate-buffered saline (PBS) without Ca^{2+} or Mg^{2+}. The resulting bone marrow cell suspensions were centrifuged at 500 *g* for 5 min at room temperature, and the BMDM pellet was resuspended in complete macrophage medium [Dulbecco's Modified Eagle medium (DMEM), 10% fetal bovine serum (FBS), 20% L-929 cell conditioned medium, 10 mM L-glutamine, 100 IU/ml penicillin and 100 μg/ml streptomycin]. BMDMs were plated into 6-well dishes (4×10^5 cells/well) in 10 ml of complete macrophage medium and incubated at 37 °C in a 5% CO_2 atmosphere. After 7 days, 5 ml of the complete macrophage medium was replaced. After another 7 days, adherent BMDMs were used in subsequent experiments. In some experiments, cultured BMDMs were treated with LPS at 0.25, 0.5, or 1.0 μg/ml. Control cultures were treated with PBS. Cell culture medium and cell pellets were assayed for assessment of target mRNA and proteins as described below.

2.4. Isolation and culture of alveolar macrophages (AMs) from mice

AMs were isolated and cultured according to the previous method [14]. The collected BALF was centrifuged at 1000*g* for 10 min and washed three times with pathogen-free PBS. The pellet was resuspended in RPMI 1640 media containing 10% fetal bovine serum (FBS) and 20 KU/L penicillin-30 KU/L streptomycin with 10% CO2 in air at 37 °C for 3.0 h.

2.5. ZBP-1 knockdown in BMDMs

Three small interfering (si) RNAs, each 20–25 nt long, targeting the ZBP-1 transcript (Dharmacon) were pooled and used as anti-ZBP-1 siRNA at a concentration of 50 nM. This siRNA cocktail was added to BMDMs in 6-well plates (2×10^6 cells/well) and the cultures were incubated in complete macrophage medium [Dulbecco's Modified Eagle medium (DMEM), 10% fetal bovine serum (FBS), 20% L-929 cell conditioned medium, 10 mM L-glutamine, 100 IU/ml penicillin and 100 μg/ml streptomycin] for 48 h and the medium was changed per 12 h, after which the treated cells were used directly for *in vitro* experiments or they were administered to mice for *in vivo* studies (see below). Down-regulation of ZBP-1 in the treated cells was confirmed by Western blotting.

2.6. Induction of ALI in mice and sample collection

ALI was induced as described [29] by intratracheal instillation of *E.coli* 055:B5 LPS (Sigma) at 2.0 mg/kg in PBS. Control mice were treated with equal volume of PBS in the same way. In some experiments, mice previously depleted of alveolar macrophages were first treated by intratracheal instillation with PBS or BMDMs (2.0×10^6 cells, 200 μl) that had been transfected with anti-ZBP1 siRNA or a scrambled siRNA control. Our preliminary data showed that intratracheal instillation with BMDMs (dosage: 2.0×10^6 cells, 200 μl) into lung of depleted mice had an proximate 86.5% retention rate and 13.5% of BMDMs were cleared. At 30 min later, these animals were treated with 2.0 mg/kg LPS by intratracheal instillation.Blood was collected from animals through a puncture in the right ventricle, and serum was obtained by centrifugation at 1800 g for 15 min at 4 °C. The right main bronchus was ligated at the bronchial bifurcation, and bronchoalveolar lavage fluid (BALF) was collected by washing the left lung adequately with ice-cold PBS until whitening was apparent. Tissue was taken from the right lung to assess pulmonary edema and histopathology. Samples of serum, BALF, and right lung tissue were stored at −80 °C until further study.

2.7. Assessment of pulmonary edema

Pulmonary edema was assessed based on the wet/dry (W/D) weight ratio. The upper and middle lobes of the right lung were wiped with filter paper, then weighed to obtain the wet weight (W). These lung tissues were dried in an oven at 60 °C for 48 h and weighed to obtain the dry weight (D).

2.8. Lung histopathology and ultrastructural examination

The lower lobe of the right lung was fixed with 10% formaldehyde and stained with hematoxylin and eosin (HE). Severity of lung injury was scored according to hemorrhage, alveolar congestion, infiltration by neutrophils and incrassation of the alveolar wall. A 5-point scoring system [14] was used: 0, minimal injury; 1, mild injury; 2, moderate injury; 3, serious injury; 4, maximal injury. Right lower lung tissue was also examined by transmission electron microscopy on a JEOL 8000 microscope (Hitachi High–Technologies, Tokyo, Japan).These lung tissues were fixed in 4% glutaraldehyde for 4 h, and then placed in 1% osmium tetroxide for 1.0 h. After washing three times with 0.1 M PBS for 15 min, the specimens was kept in 2% aqueous uranyl acetate solution for 30 min. Alcohol dehydration was carried out using 50, 70, 90% alcohol, each for 15 min, and finally dehydrated with anhydrous ethanol for 20 min. The specimens were next dehydrated with 100% acetone for 20 min. Anhydrous acetone and embedding agent were mixed in 1:1 ratio by volume and allowed to fully penetrate into the tissue blocks for 2 h, and then in 100% embedding agent for further 2 h. Utrathin (80–100 nm) lung tissue sections were stained with 4% uranium acetate for 20 min, and with lead citrate for 5 min.

2.9. Assessment of inflammatory responses in vivo

BALF was centrifuged for 10 min at 1400 g and 4 °C, cell pellets were resuspended in DMEM containing 10% FBS, and the total number of infiltrated cells was determined by hemocytometer (YA0810;

Solarbio, Beijing, China). Total protein in BALF was assayed using the bicinchoninic acid method (Pierce™ BCA Protein Assay Kit, catalog no. 23225; ThermoFisher Scientific). BALF, serum and cell culture medium were assayed for tumor necrosis factor (TNF)-α as well as interleukins (IL)-6 and IL-1β using commercial enzyme-linked immunosorbent assays (ThermoFisher Scientific) according to the manufacturer's instructions. Myeloperoxidase (MPO) activity in lung homogenates was determined using an MPO assay kit (Invitrogen) according to the manufacturer's protocol.

2.10. Gene expression in vivo using real-time quantitative polymerase chain reaction (RT-qPCR)

Total RNA was extracted from AMs and BMDMs using TRIzol reagent (Invitrogen). Single-stranded cDNAs encoding RIPK1, RIPK3, MLKL, ZBP-1, cytochrome *c* oxidase subunit IV (COX-IV), Toll-like receptor 9 (TLR9) or NF-κB were synthesized and amplified by PCR using the Takara RNA PCR kit (Takara, Dalian, China). Expression of these target genes was quantified relative to expression of glyceraldehyde 3–phosphate dehydrogenase (GAPDH). The following primers were used: RIPK1 (forward: 5′-ATG CAC GTG CTA AAG ACC CA-3′, reverse: 5′-AGG AAG CCA CAC CAA GAT CG −3′), RIPK3 (forward: 5′-CCA GAG GCC ACT TGT GTA GCG-3′, reverse: 5′-CGC TTT AGA AGC CTT CAG GTT GAC-3′), MLKL (forward: 5′-AGC CCA AAG AGG CAG CAC AAA TC-3′, reverse: 5′- AAA CTT CCA AAT ATG GGA CTT CTT G-3′), ZBP-1 (forward: 5′-AAG AGT CCC CTG CGA TTA TTT G-3′, reverse: 5′-TCT GGA TGG CGT TTG AAT TGG-3′), COX-IV (forward: 5′-TGT TGG CTA CCA GGG CAC TTA-3′, reverse: 5′- GGT AGT CAC GCC GAT CAA CAT A-3′), TLR9 (forward: 5′-GCA CCC TCC TCC AGA AAC TCG-3′, reverse: 5′-GAG AAT GTT GTG GCT GAG GTT GAC-3′), NF-κB (forward: 5′-AG G ACT TGC TGA GGG TTG G-3′, reverse: 5′-TGG GGT GGT TGA TAA GGA GTG-3′), GADPH (forward: 5′-GGC ACA GTC AAG GCT GAG AAT G-3′, reverse: 5′- ATG GTG GTG AGA CGC CAG TA-3′). The level of each target gene was normalized relative to that of β-actin in each sample using the ΔCt method. Relative differences in gene expression among groups of the lung tissues were determined using the comparative Ct (ΔΔCt) method and fold expression was calculated by the formula $2^{-\Delta\Delta Ct}$, where ΔΔCt represents ΔCt values normalized relative to the mean ΔCt of healthy control samples.

2.11. Protein levels in vivo based on Western blotting

Total protein was isolated from AMs and BMDMs using RIPA lysis buffer with protease inhibitors (Beyotime Institute of Biotechnology, Haimen, China), and the concentration of isolated protein was determined using the Pierce™ BCA Protein Assay Kit. Equal amounts of protein were fractionated by sodium dodecyl sulfate–polyacrylamide gel electrophoresis (Bio–Rad Laboratories, Hercules, CA, USA) and transferred onto polyvinylidene fluoride membranes (Bio–Rad). Membranes were incubated overnight with primary antibodies against RIPK1 (NBP1-77077; Novus Biologicals), RIPK3 (NBP1-77299; Novus), MLKL (ab187091; Abcam); ZBP-1 (NBP1-76854; Novus), COX-IV

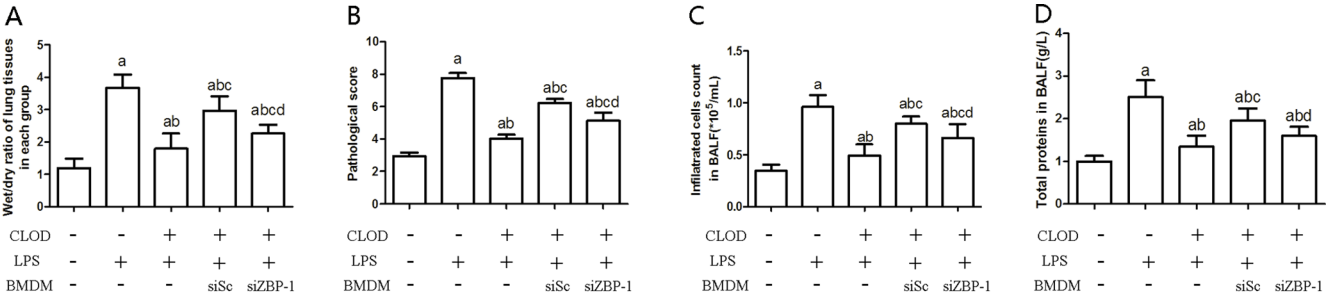

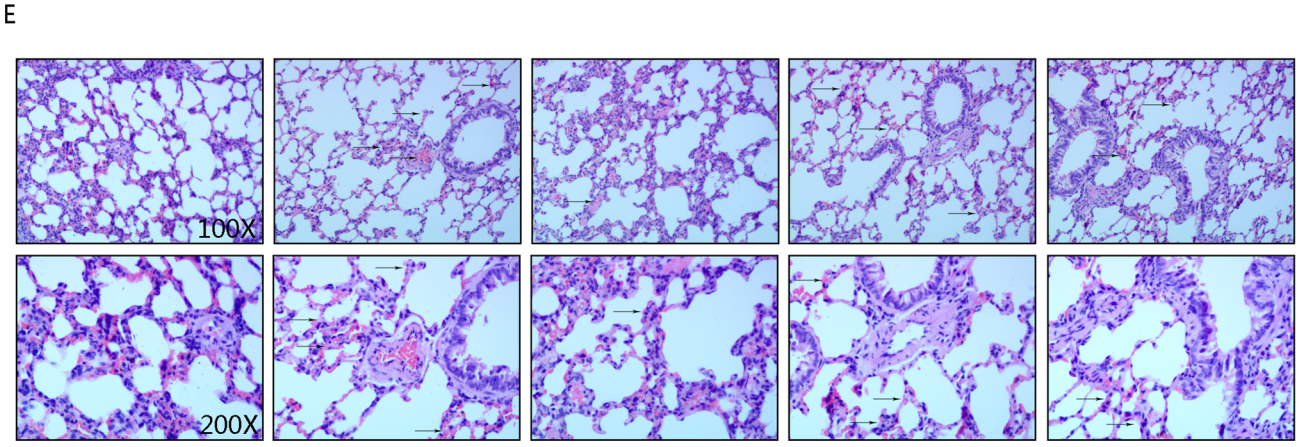

Fig. 1. Knocking down ZBP-1 in AMs attenuates LPS-induced lung injury. (A) Wet (W)/dry (D) weight ratios of lung tissues. (B) Pathological score of lung tissues, based on hematoxylin-eosin staining. (C) Total cell counts in BALF. (D) Levels of total protein in BALF. (E) Histopathologic examination for lung tissue. Hematoxylin-eosin staining showed that LPS increased inflammatory cell infifiltration (as arrow indicate), alveolar septal thickening, and pulmonary edema in the lung compared with control and CLOD mice with LPS treatment. Simultanesously the CLOD mice receiving ZBP-1-deficient BMDMs showed much milder lung pathology. All data are presented as means ± SD ($n = 6$ per group). $^{a}P < 0.05$ compared with control group (non LPS stimulated normal lungs); $^{b}P < 0.05$ compared with LPS stimulation alone group; $^{c}P < 0.05$ compared with LPS and CLOD stimulation group; $^{d}P < 0.05$ compared with siSc group. CLOD, clodronate liposomes; LPS, lipopolysaccharide; AMs, alveolar macrophages; BMDMs, bone marrow-derived macrophages; siSC, non-specific scrambled siRNA; siZBP-1, ZBP-1 siRNA.

(NBP110-39115; Novus), TLR9 (NBP2-24729; Novus), NF-κB (ab16502; Abcam) and GADPH (ab8245; Abcam). Then membranes were incubated with horseradish peroxidase-conjugated secondary antibody to allow chemiluminescent visualization (Beyotime Institute of Biotechnology) on the ChemiDoc MP system (Bio–Rad). Bands were quantitated densitometrically using in–house software developed at the Affiliated Tumor Hospital of Guangxi Medical University (Nanning, China).

2.12. Statistical analysis

Data were analyzed using SPSS 23.0 (IBM, Chicago, IL, USA) and expressed as mean ± SD. One-way ANOVA was used to assess inter–-group differences for significance, and pair-wise comparisons were assessed using the LSD-t tests. Differences associated with two-tailed $P < 0.05$ were defined as statistically significant.

3. Results

3.1. Knockdown of ZBP-1 in macrophages attenuates LPS-induced lung injury

To elucidate the role of macrophage ZBP-1 in LPS-induced lung injury, we depleted mice of AMs, gave them ZBP-1-deficient BMDMs and finally treated them with LPS. The animals showed significantly lower W/D ratio (Fig. 1A), pathological score (Fig. 1B), numbers of infiltrating cells in BALF (Fig. 1C), and protein content in BALF (Fig. 1D) than mice that received BMDMs transfected with scrambled control siRNA or mice that were not depleted of native macrophages. Similarly, the mice receiving ZBP-1-deficient BMDMs showed much milder lung pathology than the two types of control animals in terms of neutrophil infiltration in the lung parenchyma, accumulation of protein-rich fluid in the alveolar space and lung structure disorder (Fig. 1E), as well as ultrastructural defects including nuclear karyopyknosis, cell membrane disorder and organelle swelling (Fig. 2). Simultaneously, mice receiving ZBP-1-deficient BMDMs showed lower levels of IL-1β, IL-6 and TNF-α in BALF and plasma than the two types of control animals (Fig. 3A-F).

3.2. Knockdown of ZBP-1 in macrophages attenuates LPS-induced necroptosis

Mice receiving ZBP-1-deficient BMDMs showed lower expression of RIPK1 and RIPK3 and lower MLKL phosphorylation in AMs than control animals that had not been depleted of native macrophages or that had been depleted and given BMDMs transfected with a scrambled control siRNA (Fig. 4A-G). These results suggest that ZBP-1-mediated necroptosis plays an important role in LPS-induced lung injury and acute inflammation.

3.3. Knockdown of ZBP-1 in macrophages correlates with reduced levels of mtDNA, TLR9 and NF-κB

BMDMs transfected with siSC or siZBP-1 were utilized in this study. ZBP-1 expression was depleted by approximately 80% in BMDMs transfected with a specific siZBP-1 (Fig. 5A-B and 5F). Mice receiving ZBP-1-deficient BMDMs showed lower levels of the mtDNA biomarker COX-IV than the two sets of control animals (Fig. 5A, 5C and 5G), as well as lower levels of TLR9 and NF-κB/p65 (Fig. 5A, D-E and H-I).

3.4. LPS induces injury in cultured BMDMs in a concentration-dependent manner

To begin to understand the role of ZBP-1 in these *in vivo* changes in greater detail, we switched to an *in vitro* system of BMDM cultures. Treating cells with 0.25, 0.5, or 1.0 μg/ml LPS increased levels of IL-1β,

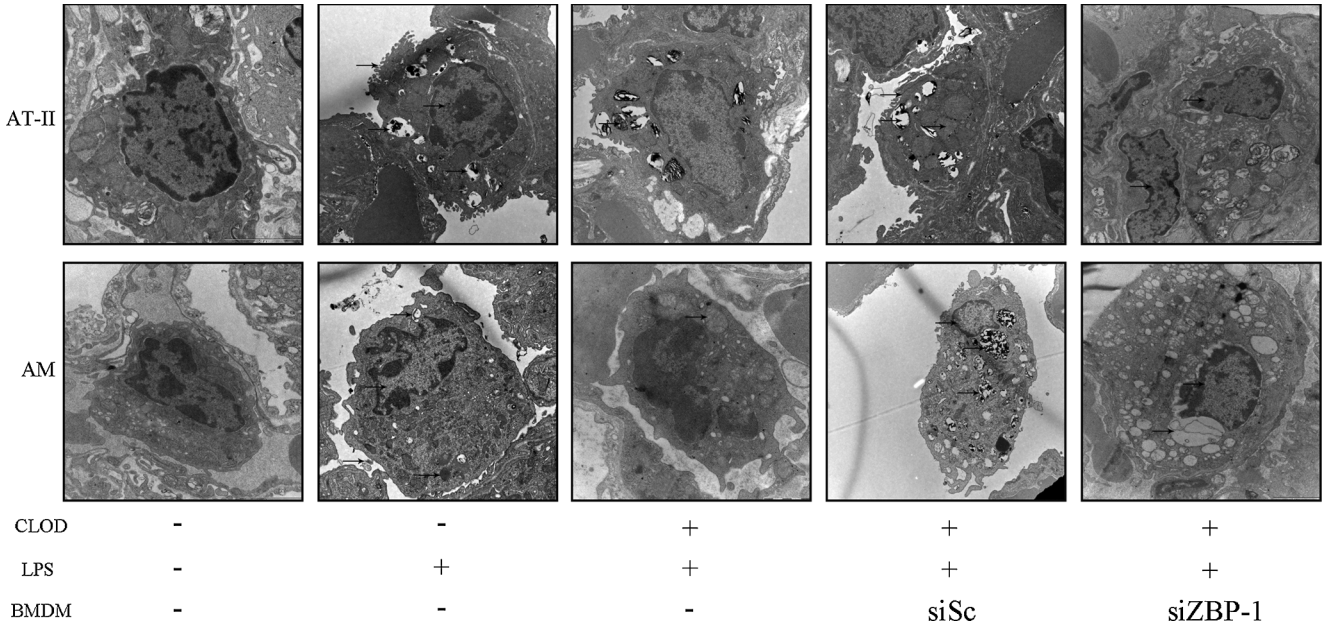

Fig. 2. Transmission electron microscopy of lungs in macrophage-depleted mice following LPS stimulation. Representative images show (A) type II lung epithelial cells (AT-II), (B) alveolar macrophages (AMs). Transmission electron microscopy showed that LPS increased nuclear karyopyknosis, cell membrane disorder and organelle swelling (as arrow indicate) in the lung compared with control and CLOD mice with LPS treatment. Simultanesously. the CLOD mice receiving ZBP-1-deficient BMDMs showed much milder lung ultrastructural defects. Scale bar, 2.0 μm. CLOD, clodronate liposomes; LPS, lipopolysaccharide; BMDMs, bone marrow-derived macrophages; siSC, non-specific scrambled siRNA; siZBP-1, ZBP-1 siRNA.

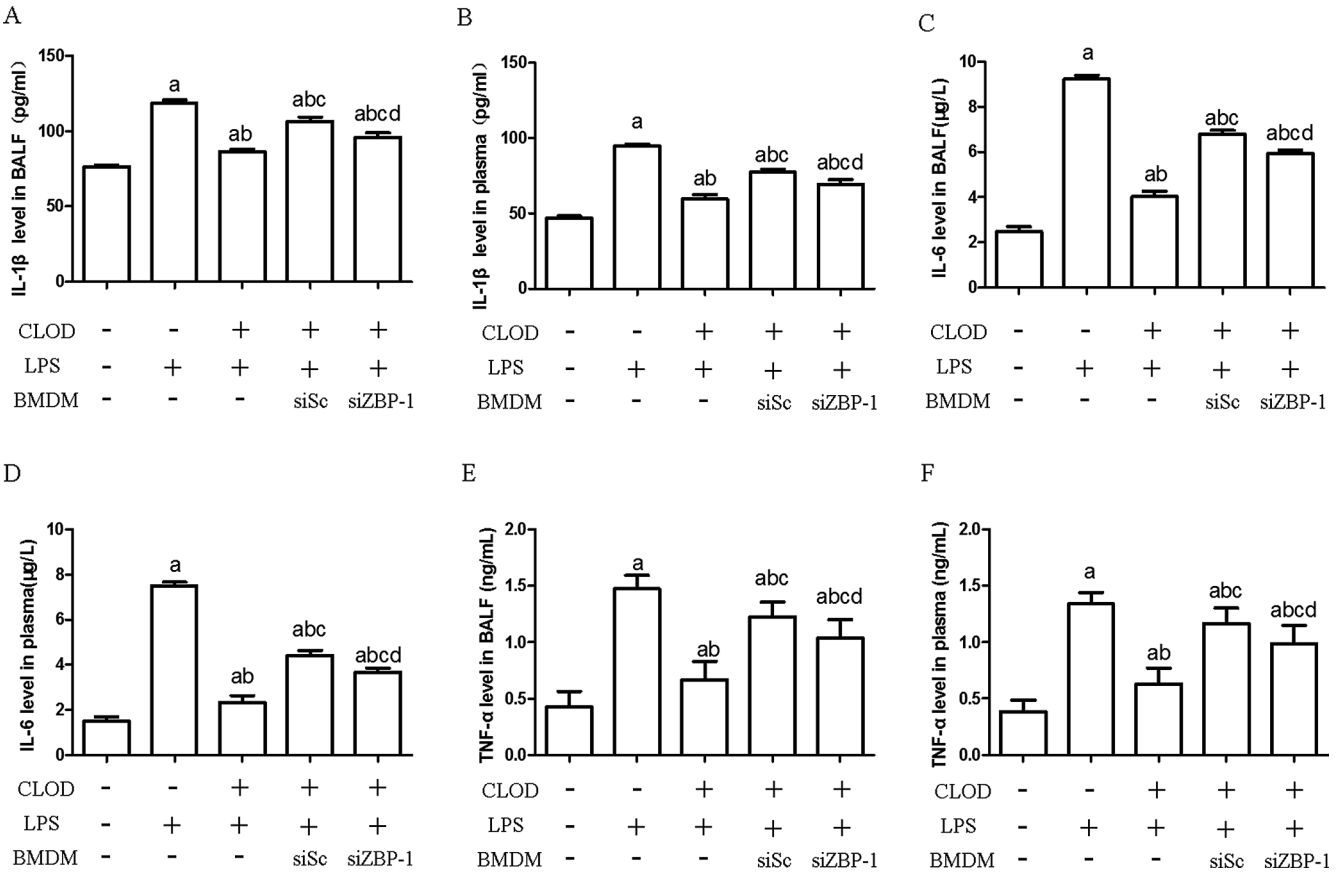

Fig. 3. ZBP-1-mediated necroptosis stimulates release of IL-1β, IL-6 and TNF-α in mouse lungs following LPS stimulation. (A) Concentration of IL-1β in BALF; (B) Concentration of IL-1β in plasma; (C) Concentration of IL-6 in BALF; (D) Concentration of IL-6 in plasma; (E) Concentration of TNF-α in BALF; (F) Concentration of TNF-α in plasma. All data are presented as means ± SD ($n = 6$ per group). [a]$P < 0.05$ compared with control group (non LPS stimulated normal lungs); [b]$P < 0.05$ compared with LPS stimulation alone group; [c]$P < 0.05$ compared with LPS and CLOD stimulation group; [d]$P < 0.05$ compared with siSc group. CLOD, clodronate liposomes; LPS, lipopolysaccharide; BMDMs, bone marrow-derived macrophages; siSC, non-specific scrambled siRNA; siZBP-1, ZBP-1 siRNA.

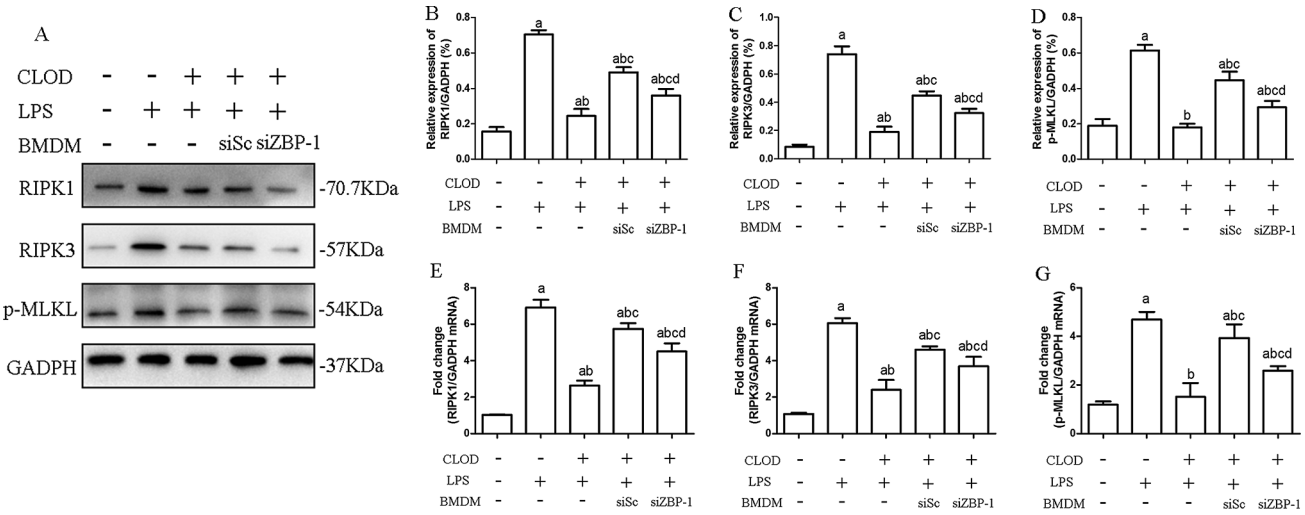

Fig. 4. Knocking down ZBP-1 in AMs mitigates LPS-induced necroptosis. (A) Expression of RIPK1, RIPK3 and p-MLKL were assessed by Western blot. (B-D) Quantifification of relative protein expression was performed by densitometric analysis and GAPDH was used as a loading control. (E-G) Relative levels of the RIPK1, RIPK3 and p-MLKL mRNAs were quantified relative to the level of GAPDH. All data are presented as means ± SD ($n = 6$ per group). [a]$P < 0.05$ compared with control group (non LPS stimulated normal lungs); [b]$P < 0.05$ compared with LPS stimulation alone group; [c]$P < 0.05$ compared with LPS and CLOD stimulation group; [d]$P < 0.05$ compared with siSc group. CLOD, clodronate liposomes; LPS, lipopolysaccharide; BMDMs, bone marrow-derived macrophages; siSC, non-specific scrambled siRNA; siZBP-1, ZBP-1 siRNA.

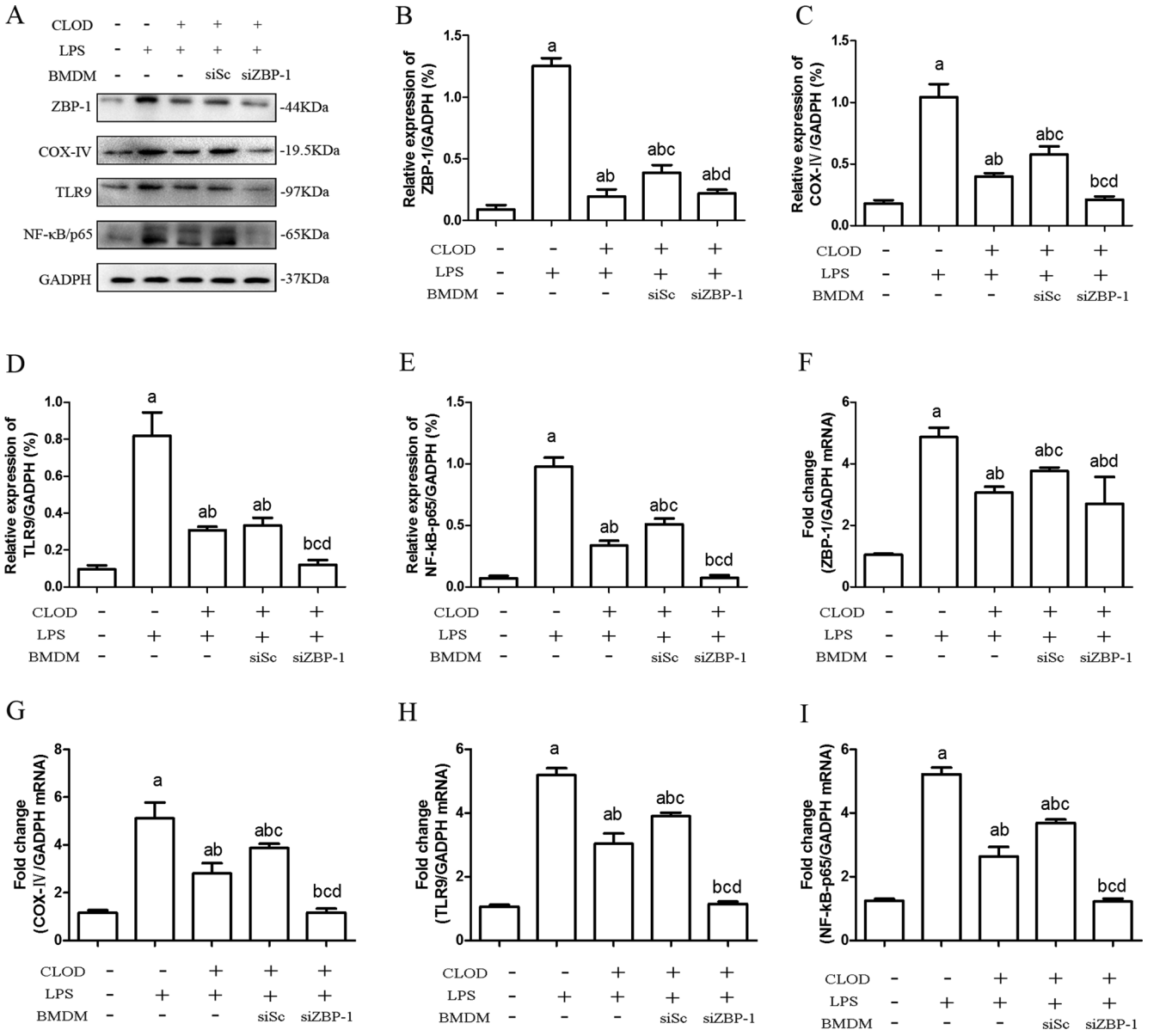

Fig. 5. ZBP-1-mediated necroptosis triggers release of mtDNA and activates the TLR9/NF-κB pathway in AMs following LPS stimulation. (A) Expression of ZBP-1, COX-IV, TLR9 and NF-κB/p65 were assessed by Western blot. (B-E) Quantifification of relative protein expression was performed by densitometric analysis and GAPDH was used as a loading control. (F-I) Relative expression of ZBP-1, COX-IV, TLR9 and NF-κB/p65 mRNA were quantified relative to the level of GAPDH. All data are presented as means ± SD ($n = 6$ per group). $^{a}P < 0.05$ compared with control group (non LPS stimulated normal lungs); $^{b}P < 0.05$ compared with LPS stimulation alone group; $^{c}P < 0.05$ compared with LPS and CLOD stimulation group; $^{d}P < 0.05$ compared with siSc group. CLOD, clodronate liposomes; LPS, lipopolysaccharide; BMDMs, bone marrow-derived macrophages; siSC, non-specific scrambled siRNA; siZBP-1, ZBP-1 siRNA.

IL-6 and TNF-α in the medium in a concentration-dependent manner (Fig. 6A-C). LPS also induced nuclear karyopyknosis, cell membrane disorder and organelle edema in a dose-dependent way (Fig. 6D). In BMDMs with silenced ZBP-1, levels of IL-1β, IL-6 and TNF-α in the medium were lack of statistical difference after treating with 0.25, 0.5, or 1.0 μg/ml LPS, which were both decreased in comparison with these inflammatory factors level in WT BMDMs (Fig. 6A-C). Simultaneously, the degree of nuclear karyopyknosis, cell membrane disorder and organelle edema were similar in treating silenced ZBP-1 BMDMs with 0.25, 0.5, or 1.0 μg/ml LPS (Fig. 6D).

3.5. LPS-induced necroptosis in cultured BMDMs involves up-regulation of RIPK1, RIPK3, p-MLKL, ZBP-1, COX-IV, TLR9 and NF-κB/p65

Treating BMDM cultures with LPS up-regulated RIPK1, RIKP3 and p-MLKL in a roughly concentration-dependent manner, which were aborted in silenced ZBP-1 BMDMs (Fig. 7A-H). Levels of RIKP3 and p-MLKL were similar between WT BMDMs and silenced ZBP-1 BMDMs treated with 0.25 μg/ml LPS and untreated control cells (Fig. 7A-B, D-F and G-H).

LPS also up-regulated ZBP-1 at higher LPS concentrations (Fig. 8A, C and G), and it induced higher levels of COX-IV, TLR9 and NF-κB/p65

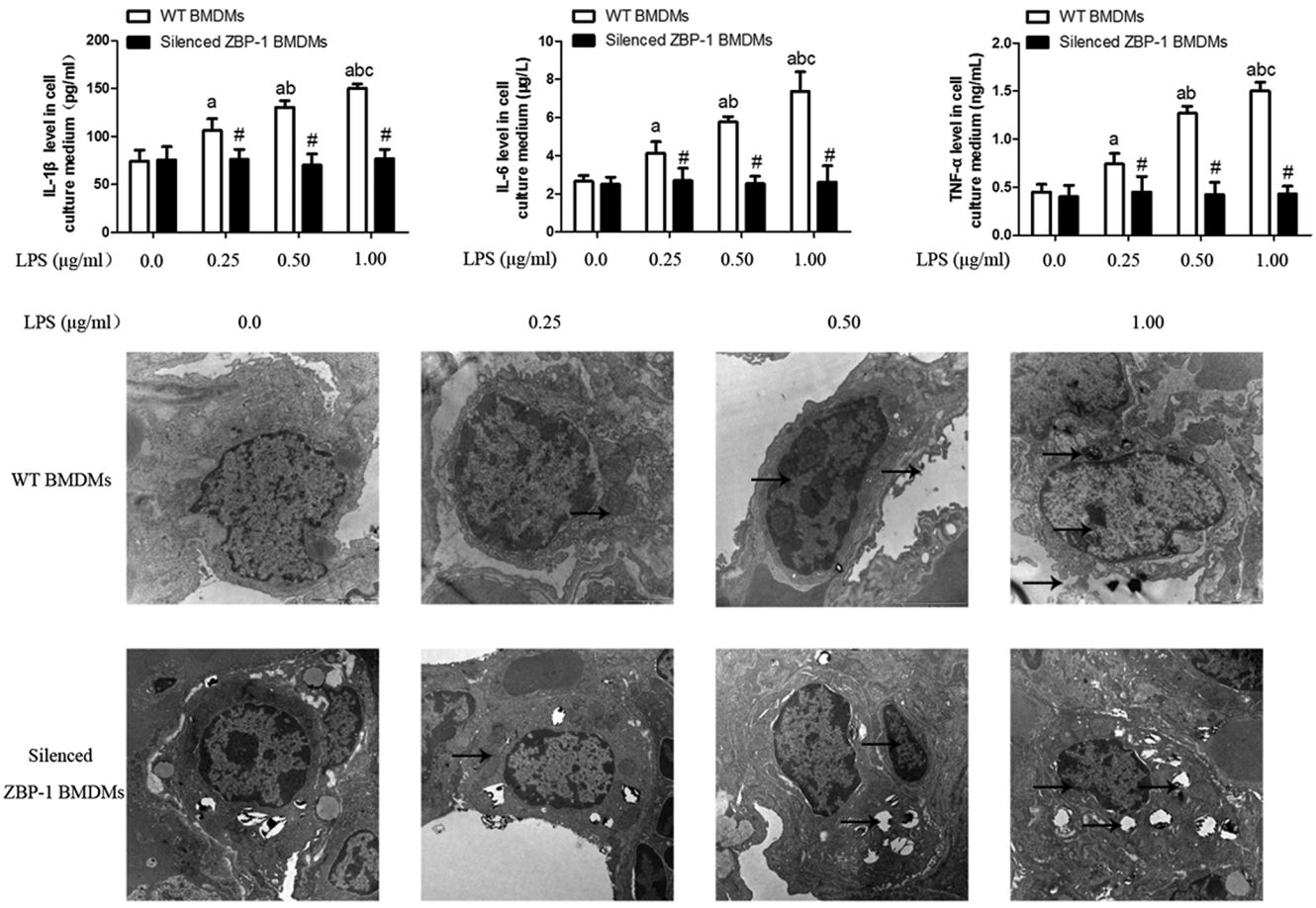

Fig. 6. LPS treatment induces release of IL-1β, IL-6 and TNF-α and cell injury in cultured BMDMs. (A) Concentration of IL-1β in cell culture medium. (B) Concentration of IL-6 in cell culture medium. (C) Concentration of TNF-α in cell culture medium. (D) Representative images of BMDMs with or without silenced ZBP-1following 0.25, 0.50 and 1.00 μg/ml LPS treatment. All data are presented as means ± SD (Cell counts = $5*10^9$ per group). $^{a}P < 0.05$ compared with control group (non LPS stimulated BMDMs); $^{b}P < 0.05$ compared with 0.25 μg/ml of LPS stimulation group; $^{c}P < 0.05$ compared with 0.50 μg/ml of LPS stimulation group; $^{\#}P < 0.05$ compared with BMDMs without silenced ZBP-1. WT BMDMs, bone marrow-derived macrophages without silenced ZBP-1; Silenced ZBP-1 BMDMs, bone marrow-derived macrophages with silenced ZBP-1.

in a concentration-dependent manner (Fig. 8A, D-F and H-J). However, LPS did not induce the up-regulation of COX-IV, TLR9 and NF-κB/p65 in silenced ZBP-1 BMDMs treating with 0.25, 0.5, or 1.0 μg/ml LPS (Fig. 8B, D-F and H-J). These results suggest that LPS induces necroptosis by activating ZBP-1, which in turn activates the mtDNA/TLR4/NF-κB pathway and silenced ZBP-1 in BMDMs can stop the pathway *in vitro*.

4. Discussion

Using a mouse model of ALI, we provide evidence that ZBP-1-mediated necroptosis in macrophages contributes to LPS-induced lung injury. Knockdown of ZBP-1 in macrophages abolished LPS-induced necroptosis, pro-inflammatory cytokine release, as well as lung inflammation and injury. Building on these *in vivo* experiments, we showed *in vitro* that LPS-induced injury correlates with up-regulation of ZBP-1 as well as the mtDNA/TLR4/NF-κB pathway. These results provide testable hypotheses to further understand how ALI arises and what proteins may be targeted to prevent or mitigate it.

One of the main findings of this study is the identification of macrophages as a key target for ZBP-1 mediated necroptosis induced by LPS. This finding is based on the following evidence. First, LPS significantly increased levels of RIPK1, RIPK3 and p-MLKL in lung macrophages, and depleting alveolar macrophages dramatically reduced LPS-induced necroptosis in the lung. Furthermore, silencing ZBP-1 in BMDMs and administering them to macrophage-depleted mice dramatically attenuated LPS-induced inflammation and lung injury. These results suggest that macrophages are a necroptosis "sensor" of LPS. We confirmed these *in vivo* findings by showing that LPS treatment of BMDM cultures strongly activated ZBP-1-mediated necroptosis.

LPS has already been shown to activate RIP3-mediated necroptosis in severe acute respiratory distress syndrome (ARDS), stimulating the NLRP3 inflammasome [2,28]. Several studies suggest that necroptosis also contributes to ALI. Studies in humans and animals suggest that ventilator-induced lung injury up-regulates RIPK3, and studies in mice indicate that reducing RIPK3 levels ameliorates such lung injury [24]. The ability of insulin-like growth factor-1 inhibition to attenuate LPS-induced lung injury also appears to involve the ability to down-regulate RIPK3 [11]. Our data extend the literature by showing that necroptosis mediates LPS-induced lung inflammatory injury, and that this involves up-regulation of ZBP-1 in macrophages.

In this study, we found that COX-IV, TLR9 and NF-κB/p65 level

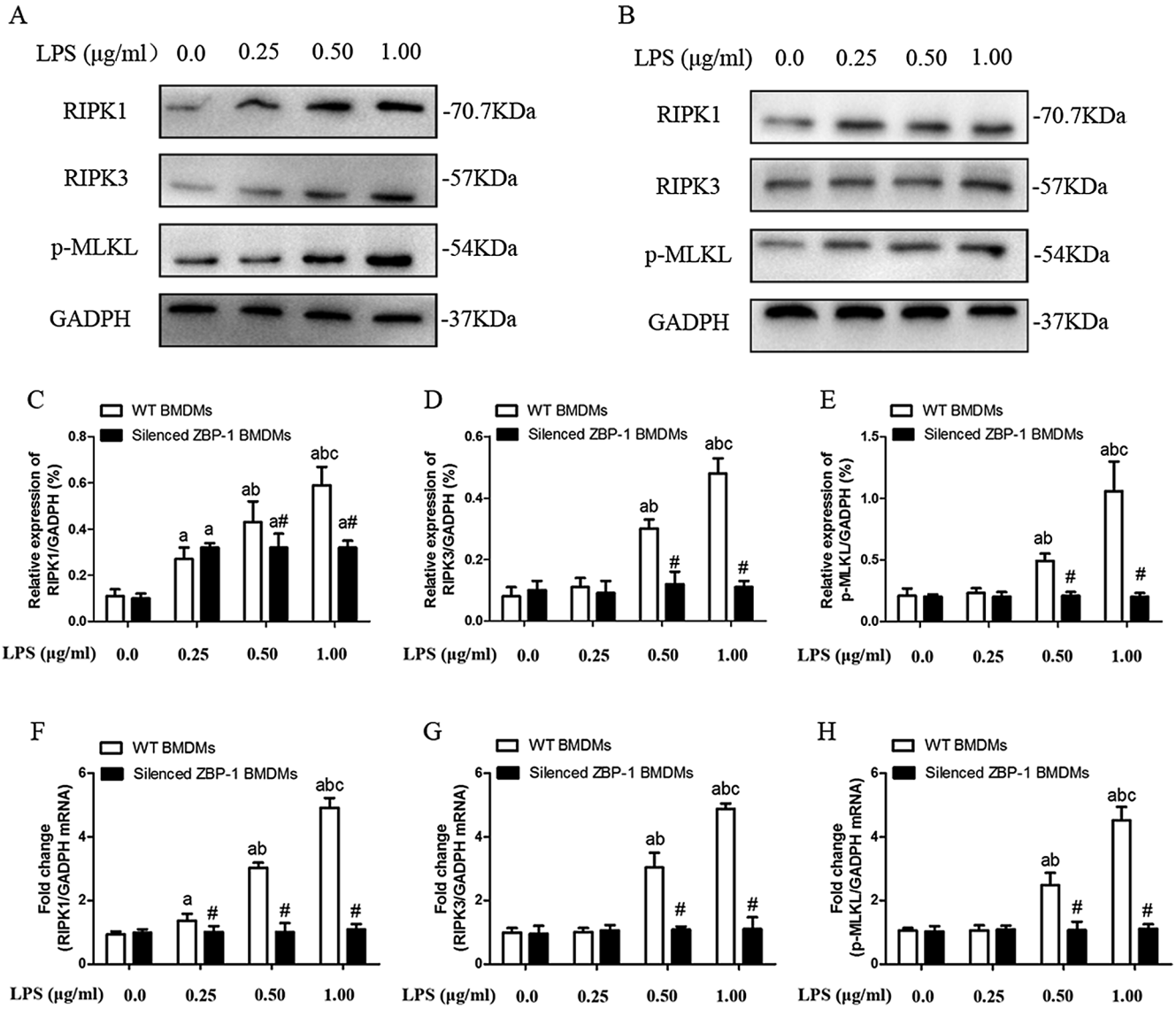

Fig. 7. LPS treatment induces necroptosis in cultured BMDMs. (A) Expression of RIPK1, RIPK3 and p-MLKL in BMDMs without silenced ZBP-1 were assessed by Western blot. (B) Expression of RIPK1, RIPK3 and p-MLKL in BMDMs without silenced ZBP-1 were assessed by Western blot. (C-E) Quantifification of relative protein expression was performed by densitometric analysis and GAPDH was used as a loading control. (E-G) Relative levels of the RIPK1, RIPK3 and p-MLKL mRNAs were quantified relative to the level of GAPDH. All data are presented as means ± SD (Cell counts = $5 * 10^9$ per group). $^{a}P < 0.05$ compared with control group (non LPS stimulated BMDMs); $^{b}P < 0.05$ compared with 0.25 μg/ml of LPS stimulation group; $^{c}P < 0.05$ compared with 0.50 μg/ml of LPS stimulation group; $^{\#}P < 0.05$ compared with BMDMs without silenced ZBP-1. WT BMDMs, bone marrow-derived macrophages without silenced ZBP-1; Silenced ZBP-1 BMDMs, bone marrow-derived macrophages with silenced ZBP-1.

were up-regulated in mice subjected to LPS after receiving BMDMs in which ZBP-1 was knocked down. ZBP-1-mediated necroptosis may drive ALI by releasing mtDNA and potentially other intracellular damage-associated molecular patterns [20,22], which activate the TLR9/NF-κB pathway. Necroptosis, in contrast to apoptosis and autophagy, involves rupture of the cell membrane and release of cellular contents that activate inflammation [13]. Indeed, our previous studies showed that in ventilation-induced lung inflammation and injury, mitophagy is activated and releases mtDNA, which activates the TLR9/NF-κB pathway [9,14]. Analogously, mtDNA in transfusion products can trigger ARDS [25].

Our results suggest that LPS activates ZBP-1 expression and signals assembly of RIPK1, RIPK3 and p-MLKL to activate necroptosis, leading to the release of mtDNA and activation of TLR9/ NF-κB pathway. Future work should further clarify how ZBP-1 mediates necroptosis and how the subsequent signaling pathways contribute to inflammatory injury. An important tool in such studies will be a ZBP-1-knockout mouse.

Compliance with ethical standards

This study was done according to the NIH Guide for the Care and Use of Laboratory Animals (NIH Publication, 8th Edition. Revised 2011). The care and use of wild type C57BL/6J male mice were approved by the Institutional Animal Care and Use Committee of Guangxi Medical University.

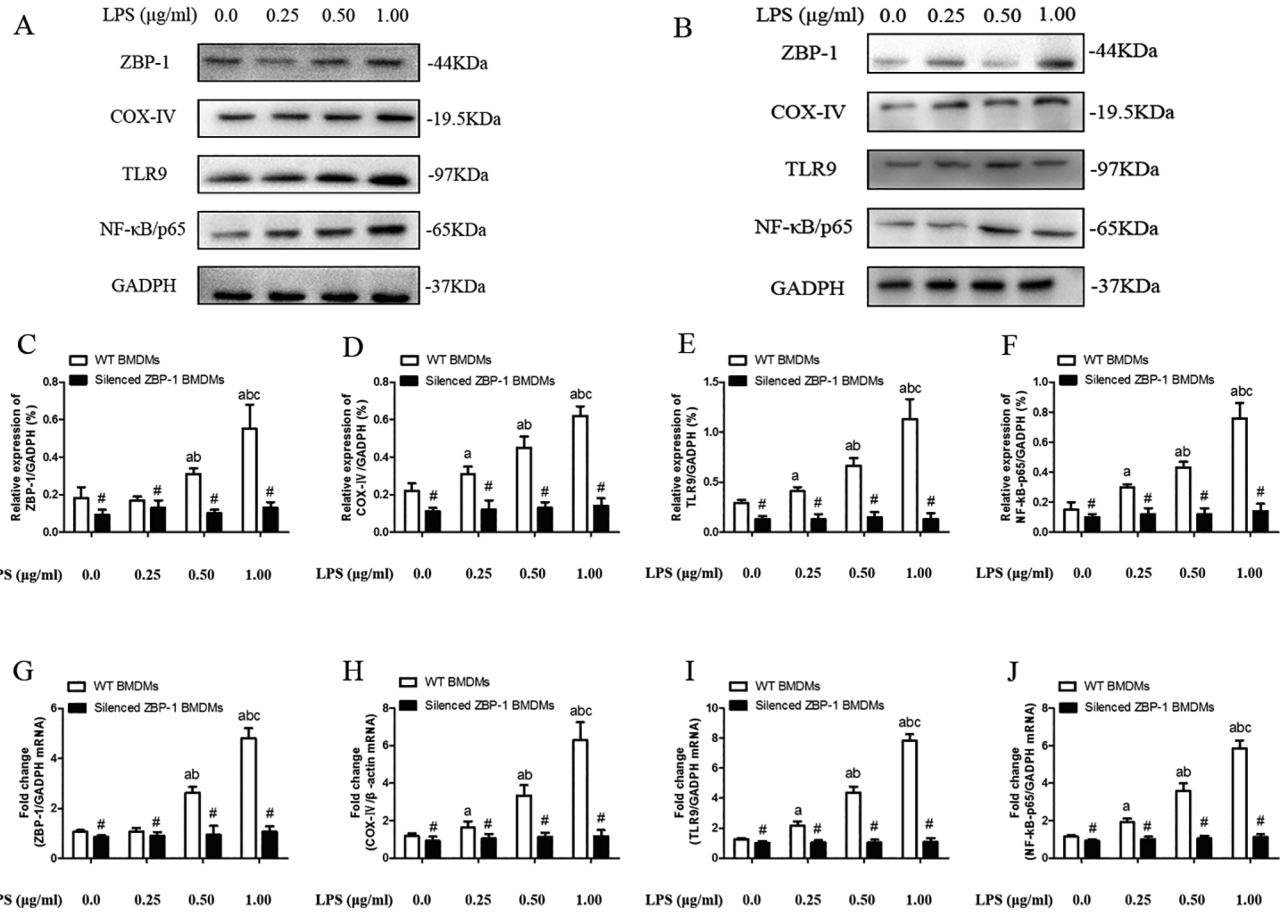

Fig. 8. ZBP-1 mediated necroptosis triggers release of mtDNA and activates the TLR9/NF-κB pathway in cultured BMDMs following LPS stimulation. (A) Expression of ZBP-1, COX-IV, TLR9 and NF-κB/p65 in BMDMs without silenced ZBP-1 were assessed by Western blot. (B) Expression of ZBP-1, COX-IV, TLR9 and NF-κB/p65 in BMDMs with silenced ZBP-1 were assessed by Western blot. (C-F) Quantifification of relative protein expression was performed by densitometric analysis and GAPDH was used as a loading control. (G-J) Relative levels of the ZBP-1, COX-IV, TLR9 and NF-κB/p65 mRNAs were quantified relative to the level of GAPDH. All data are presented as means ± SD (Cell counts = $5 * 10^9$ per group). $^{a}P < 0.05$ compared with control group (non LPS stimulated BMDMs); $^{b}P < 0.05$ compared with 0.25 μg/ml of LPS stimulation group; $^{c}P < 0.05$ compared with 0.50 μg/ml of LPS stimulation group; $^{\#}P < 0.05$ compared with BMDMs without silenced ZBP-1. WT BMDMs, bone marrow-derived macrophages without silenced ZBP-1; Silenced ZBP-1 BMDMs, bone marrow-derived macrophages with silenced ZBP-1.

Funding

This study was supported by the Guangxi Natural Science Foundation Program (2018GXNSFAA138007), the Basic Ability Improvement Project of Young Teachers in Guangxi Colleges and Universities (2018KY0113) and the Health Technology Research and Development Project of Guangxi Zhuang Autonomous Region (S2018104).

Declaration of Competing Interest

No potential conflicts of interest relevant to this article were reported.

Appendix A. Supplementary material

Supplementary data to this article can be found online at https://doi.org/10.1016/j.intimp.2019.105944.

References

[1] A. Adameova, E. Goncalvesova, A. Szobi, N.S. Dhalla, Necroptotic cell death in failing heart: relevance and proposed mechanisms, Heart Fail. Rev. 21 (2016) 213–221.
[2] J. Chen, S. Wang, R. Fu, M. Zhou, T. Zhang, W. Pan, N. Yang, Y. Huang, RIP3 dependent NLRP3 inflammasome activation is implicated in acute lung injury in mice, J. Transl. Med. 16 (2018) 233.
[3] X. Chen, Y. Zhang, W. Wang, Z. Liu, J. Meng, Z. Han, Mesenchymal stem cells modified with heme oxygenase-1 have enhanced paracrine function and attenuate lipopolysaccharide-induced inflammatory and oxidative damage in pulmonary microvascular endothelial cells, Cellular Physiol. Biochem.: Int. J. Exp. Cellular Physiol., Biochem., Pharmacol. 49 (2018) 101–122.
[4] K.T. Cheng, S. Xiong, Z. Ye, Z. Hong, A. Di, K.M. Tsang, X. Gao, S. An, M. Mittal, S.M. Vogel, E.A. Miao, J. Rehman, A.B. Malik, Caspase-11-mediated endothelial pyroptosis underlies endotoxemia-induced lung injury, J. Clin. Investig. 127 (2017) 4124–4135.
[5] L. de Almeida, A. Dorfleutner, C. Stehlik, In vivo analysis of neutrophil infiltration during LPS-induced peritonitis, Bio-protocol 6 (2016).
[6] A. Degterev, Z. Huang, M. Boyce, Y. Li, P. Jagtap, N. Mizushima, G.D. Cuny, T.J. Mitchison, M.A. Moskowitz, J. Yuan, Chemical inhibitor of nonapoptotic cell death with therapeutic potential for ischemic brain injury, Nat. Chem. Biol. 1 (2005) 112–119.
[7] J. Han, C.Q. Zhong, D.W. Zhang, Programmed necrosis: backup to and competitor with apoptosis in the immune system, Nat. Immunol. 12 (2011) 1143–1149.
[8] Q. Jiang, M. Yi, Q. Guo, C. Wang, H. Wang, S. Meng, C. Liu, Y. Fu, H. Ji, T. Chen, Protective effects of polydatin on lipopolysaccharide-induced acute lung injury through TLR4-MyD88-NF-kappaB pathway, Int. Immunopharmacol. 29 (2015) 370–376.
[9] R. Jing, L. Pan, Role and mechanism of mitophagy in ventilator-induced lung injury in rats, Zhonghua wei zhong bing ji jiu yi xue 29 (2017) 6–10.
[10] A. Kaczmarek, P. Vandenabeele, D.V. Krysko, Necroptosis: the release of damage-associated molecular patterns and its physiological relevance, Immunity 38 (2013) 209–223.
[11] S.H. Lee, J.H. Shin, J.H. Song, A.Y. Leem, M.S. Park, Y.S. Kim, J. Chang, K.S. Chung, Inhibition of insulin-like growth factor receptor-1 reduces necroptosis-related markers and attenuates LPS-induced lung injury in mice, Biochem. Biophys. Res. Commun. 498 (2018) 877–883.
[12] K. Li, Z. He, X. Wang, M. Pineda, R. Chen, H. Liu, K. Ma, H. Shen, C. Wu, N. Huang, T. Pan, Y. Liu, J. Guo, Apigenin C-glycosides of Microcos paniculata protects lipopolysaccharide induced apoptosis and inflammation in acute lung injury through

TLR4 signaling pathway, Free Radical Biol. Med. 124 (2018) 163–175.
[13] J. Lin, S. Kumari, C. Kim, T.M. Van, L. Wachsmuth, A. Polykratis, M. Pasparakis, RIPK1 counteracts ZBP1-mediated necroptosis to inhibit inflammation, Nature 540 (2016) 124–128.
[14] J.Y. Lin, R. Jing, F. Lin, W.Y. Ge, H.J. Dai, L. Pan, High Tidal Volume Induces Mitochondria Damage and Releases Mitochondrial DNA to Aggravate the Ventilator-Induced Lung Injury, Front. Immunol. 9 (2018) 1477.
[15] H. Lv, Q. Liu, Z. Wen, H. Feng, X. Deng, X. Ci, Xanthohumol ameliorates lipopolysaccharide (LPS)-induced acute lung injury via induction of AMPK/GSK3beta-Nrf2 signal axis, Redox Biol 12 (2017) 311–324.
[16] K. Mizumura, S. Maruoka, Y. Gon, A.M. Choi, S. Hashimoto, The role of necroptosis in pulmonary diseases, Respirat. Invest. 54 (2016) 407–412.
[17] J.E. Morgan, A. Prola, V. Mariot, V. Pini, J. Meng, C. Hourde, J. Dumonceaux, F. Conti, F. Relaix, F.J. Authier, L. Tiret, F. Muntoni, M. Bencze, Necroptosis mediates myofibre death in dystrophin-deficient mice, Nat. Commun. 9 (2018) 3655.
[18] K. Newton, K.E. Wickliffe, A. Maltzman, D.L. Dugger, A. Strasser, V.C. Pham, J.R. Lill, M. Roose-Girma, S. Warming, M. Solon, H. Ngu, J.D. Webster, V.M. Dixit, RIPK1 inhibits ZBP1-driven necroptosis during development, Nature 540 (2016) 129–133.
[19] T. Oka, S. Hikoso, O. Yamaguchi, M. Taneike, T. Takeda, T. Tamai, J. Oyabu, T. Murakawa, H. Nakayama, K. Nishida, S. Akira, A. Yamamoto, I. Komuro, K. Otsu, Mitochondrial DNA that escapes from autophagy causes inflammation and heart failure, Nature 485 (2012) 251–255.
[20] M. Pasparakis, P. Vandenabeele, Necroptosis and its role in inflammation, Nature 517 (2015) 311–320.
[21] J.S. Pearson, C. Giogha, S. Muhlen, U. Nachbur, C.L. Pham, Y. Zhang, J.M. Hildebrand, C.V. Oates, T.W. Lung, D. Ingle, L.F. Dagley, A. Bankovacki, E.J. Petrie, G.N. Schroeder, V.F. Crepin, G. Frankel, S.L. Masters, J. Vince, J.M. Murphy, M. Sunde, A.I. Webb, J. Silke, E.L. Hartland, EspL is a bacterial cysteine protease effector that cleaves RHIM proteins to block necroptosis and inflammation, Nat. Microbiol. 2 (2017) 16258.
[22] S.D. Pouwels, G.J. Zijlstra, M. van der Toorn, L. Hesse, R. Gras, N.H. Ten Hacken, D.V. Krysko, P. Vandenabeele, M. de Vries, A.J. van Oosterhout, I.H. Heijink, M.C. Nawijn, Cigarette smoke-induced necroptosis and DAMP release trigger neutrophilic airway inflammation in mice, Am. J. Physiol. Lung Cell. Mol. Physiol. 310 (2016) L377–386.
[23] S.T. Schafer, L. Franken, M. Adamzik, B. Schumak, A. Scherag, A. Engler, N. Schonborn, J. Walden, S. Koch, H.A. Baba, J. Steinmann, A.M. Westendorf, J. Fandrey, T. Bieber, C. Kurts, S. Frede, J. Peters, A. Limmer, Mitochondrial DNA: An Endogenous Trigger for Immune Paralysis, Anesthesiology 124 (2016) 923–933.
[24] I.I. Siempos, K.C. Ma, M. Imamura, R.M. Baron, L.E. Fredenburgh, J.W. Huh, J.S. Moon, E.J. Finkelsztein, D.S. Jones, M.T. Lizardi, E.J. Schenck, S.W. Ryter, K. Nakahira, A.M. Choi, RIPK3 mediates pathogenesis of experimental ventilator-induced lung injury, JCI insight 3 (2018).
[25] J.D. Simmons, Y.L. Lee, V.M. Pastukh, G. Capley, C.A. Muscat, D.C. Muscat, M.L. Marshall, S.B. Brevard, M.N. Gillespie, Potential contribution of mitochondrial DNA damage associated molecular patterns in transfusion products to the development of acute respiratory distress syndrome after multiple transfusions, J. Trauma Acute Care Surg. 82 (2017) 1023–1029.
[26] K. Sun, R. Huang, L. Yan, D.T. Li, Y.Y. Liu, X.H. Wei, Y.C. Cui, C.S. Pan, J.Y. Fan, X. Wang, J.Y. Han, Schisandrin attenuates lipopolysaccharide-induced lung injury by regulating TLR-4 and Akt/FoxO1 signaling pathways, Front. Physiol. 9 (2018) 1104.
[27] J.W. Upton, W.J. Kaiser, DAI another way: necroptotic control of viral infection, Cell Host Microbe 21 (2017) 290–293.
[28] L. Wang, T. Wang, H. Li, Q. Liu, Z. Zhang, W. Xie, Y. Feng, T. Socorburam, G. Wu, Z. Xia, Q. Wu, Receptor interacting protein 3-mediated necroptosis promotes lipopolysaccharide-induced inflammation and acute respiratory distress syndrome in mice, PLoS ONE 11 (2016) e0155723.
[29] H. Zhang, S. Chen, M. Zeng, D. Lin, Y. Wang, X. Wen, C. Xu, L. Yang, X. Fan, Y. Gong, H. Zhang, X. Kong, Apelin-13 Administration Protects Against LPS-Induced Acute Lung Injury by Inhibiting NF-kappaB Pathway and NLRP3 Inflammasome Activation, Cellular Physiol. Biochem.: Int. J. Exp. Cellular Physiol., Biochem., Pharmacol. 49 (2018) 1918–1932.
[30] Y. Zhang, G. Liu, R.O. Dull, D.E. Schwartz, G. Hu, Autophagy in pulmonary macrophages mediates lung inflammatory injury via NLRP3 inflammasome activation during mechanical ventilation, Am. J. Physiol. Lung Cell. Mol. Physiol. 307 (2014) L173–185.